Journal of Alloys and Compounds 623 (2015) 454–459

Contents lists available at ScienceDirect

Journal of Alloys and Compounds

journal homepage: www.elsevier.com/locate/jalcom

Short range order in Ge–As–Se glasses

I. Pethes [a], I. Kaban [b,c], R.-P. Wang [d], B. Luther-Davies [d], P. Jóvári [a,*]

[a] Institute for Solid State Physics and Optics, Wigner Research Centre for Physics, P.O. Box 49, 1525 Budapest, Hungary
[b] IFW Dresden, Institute for Complex Materials, P.O. Box 270116, 01171 Dresden, Germany
[c] TU Dresden, Institute of Materials Science, 01062 Dresden, Germany
[d] Centre for Ultrahigh Bandwidth Devices for Optical Systems (CUDOS), Laser Physics Centre, Research School of Physics and Engineering, Australian National University, Canberra, ACT 0200, Australia

ARTICLE INFO

Article history:
Received 30 May 2014
Received in revised form 29 October 2014
Accepted 1 November 2014
Available online 13 November 2014

Keywords:
Chalcogenide glasses
Ge–As–Se
Structure
XRD
EXAFS
RMC

ABSTRACT

The structure of $Ge_xAs_{10}Se_{90-x}$ (x = 10, 17.5, 22.5, 27.5, 30, 35) glasses as well as some other compositions extensively used in infrared optics, e.g. GASIR®($Ge_{22}As_{20}Se_{58}$) and AMTIR-1 ($Ge_{33}As_{12}Se_{55}$) has been investigated by X-ray diffraction (XRD) and extended X-ray absorption fine structure (EXAFS) measurements at the Ge, As and Se K-edges. Structural models have been obtained by fitting simultaneously XRD and EXAFS data by the reverse Monte Carlo simulation technique. Unlike other IV–V–VI glasses (e.g. Ge–As–S, Ge–Sb–Te, Ge–Sb–Se, Ge–As–Te) Ge–As–Se glasses are characterized by the lack of preferential bonding and behave as random covalent networks: Ge–Ge, Ge–As or As–As bonds can be found in Se-rich compositions while Se–Se bonding remains in strongly Se-deficient glasses as well.

1. Introduction

In the last few years chalcogenide glasses have received renewed attention because of their prominent optical properties: low optical absorption in the mid infrared region and high linear and nonlinear refractive indices [1,2]. Chalcogenide glasses have nonlinearity several orders of magnitude greater than silica glass, which makes them useful for all-optical processing of telecommunication signals at extreme speeds [3,4]. Chalcogenide glass optical fibers are employed in numerous devices, for example in IR optical fiber lasers and amplifiers [5,6], Raman lasers [7,8] or fiber-based chemical and biomedical sensor devices [9–12]. Several other applications were considered, such as medical endoscopy [13], environmental metrology [14] or spatial interferometry. Single mode fibers, operating in the 4–20 μm range were proposed for space research in the frame of the Darwin mission [15].

Among the different families of chalcogenide glasses, the Ge–As–Se system is particularly interesting due to its very broad glass formation region, which also means the tunability of their physical and optical properties by the chemical composition. The most important parameter characterizing a chalcogenide glassy network is the mean coordination number MCN, defined as the sum of the respective elemental concentrations times their coordination number. Many physical properties of chalcogenide glasses have been found to correlate with the MCN. A transition at MCN around 2.4 from an underconstrained 'floppy' to an overconstrained 'rigid' network has been found by mean field theory using constraint counting [16,17]. Tanaka suggested that a second transition from a topologically two-dimensional structure to a three-dimensional network may occur at the average coordination number of 2.67 [18]. A large number of experiments demonstrated that many chemical and physical properties change abruptly at these MCN values [19,20]. Random networks, in which stressed configurations are avoided if possible, show two transitions and an intermediate state that is rigid but stress-free [21]. By temperature-modulated differential scanning calorimetry and Raman scattering measurements a thermally reversing compositional window was reported, where the glasses are generally non-aging [22,23].

To assess the validity of mean field approximations and to learn more about the structure of Ge–As–Se glasses in general, it is essential to know their chemical short range order. Compositions with 5 and 15 at.% Ge have been studied recently [24] by fitting X-ray diffraction measurements simultaneously with Ge, As and Se K-edge extended X-ray absorption fine structure (EXAFS) datasets in the framework of the reverse Monte Carlo simulation technique (RMC) [25–27]. It has been found that the glasses investigated (with values of MCN up to 2.64) can be characterized as random covalent networks: bonds between Ge and As (Ge–Ge,

* Corresponding author.

http://dx.doi.org/10.1016/j.jallcom.2014.11.002
0925-8388/

As–As, As–Ge) can be found in compositions with excess Se while Se–Se bonds persist in the strongly Se-deficient region.

It is important to know whether the lack of chemical short range order is characteristic of low (5–15%) Ge content glasses only or persists over a wider composition range. For this reason we investigate the structure of Ge–As–Se glasses up to 35% Ge content. Similarly to our previous study, large scale structural models are obtained by fitting simultaneously X-ray diffraction and EXAFS measurements (4 datasets for each composition) with the reverse Monte Carlo technique. Short range order parameters (bond lengths, coordination numbers) are discussed in detail and compared with those of other IV–V–VI glasses.

2. Experimental details

The X-ray diffraction measurements of $Ge_{22}As_{20}Se_{58}$, $Ge_{33}As_{12}Se_{55}$ and $Ge_{33}As_{20}Se_{47}$ were carried out at the BW5 experimental station at HASYLAB (DESY, Hamburg, Germany). The Ge, As and Se K-edge EXAFS spectra of the above compositions and those of the $Ge_xAs_{10}Se_{90-x}$ (x = 10, 22.5, 27.5, 30, 35) series were measured at beamline X1 of HASYLAB. For the details of the above experiments and that of the sample preparation we refer to some recent publications [24,28]. Glass compositions were determined using energy dispersive spectroscopy. Polished samples were measured at three different positions and the results were averaged. The difference between the nominal and the experimental compositions is less than 0.5%.

X-ray diffraction structure factors of the $Ge_xAs_{10}Se_{90-x}$ glasses were measured at the P07 high energy materials science beamline [29] at PETRA III synchrotron storage ring (DESY, Hamburg, Germany). The radiation of the undulator source was monochromatized by a double crystal monochromator consisting of two bent Si(1 1 1) Laue crystals. The energy of the monochromatic radiation was 100.0 keV. Bulk pieces of Ge–As–Se glasses (1–1.5 mm thickness) were measured in transmission mode. Each sample was illuminated for 10 × 5 s. The size of the incident beam was 0.25 × 0.25 mm^2.

Scattered intensities were measured by a 2D detector (Perkin–Elmer XRD 1622). The sample-detector distance was 289.4 mm. Raw intensities were corrected for background and polarization and integrated to Q-space by the program Fit2D [30]. The integrated data were corrected for Compton-scattering [31]. Some selected structure factors $S(Q)$ and the corresponding k^3-weighted $\chi(k)$ curves are shown in Figs. 1 and 2.

3. Reverse Monte Carlo simulation

Model configurations were obtained by fitting simultaneously the Ge, As, Se K-edge EXAFS data and the XRD structure factor for each composition. Though RMC was used first with diffraction data [25] it was practically immediately implemented for EXAFS [32]. Technical details of using EXAFS data in RMC modeling are discussed in Refs. [27,33].

Simulation boxes contained 20,000 atoms. Densities were taken from Refs. [19,28]. Initial configurations were obtained in two steps: (1) atoms were placed at random in the simulation box; (2) atoms were moved around until their separations were higher than the minimum interatomic distances. The minimum interatomic distances were usually equal to 2.2 Å if bonding was allowed and 2.9 Å in case of forbidden bonds (see e.g. 4.2). The maximum random displacement was 0.1 Å along each coordinate. In accordance with the '8-N' rule [34], the *total* coordination numbers of Ge, As and Se were forced to be 4, 3 and 2, respectively. N_i, the total coordination number of the ith component is defined as the sum of N_{ij}, the average number of j type neighbors around i type atoms. We note here that the validity of the '8-N' rule in IV–V–VI glasses have been confirmed by several studies [35–38]. The above coordination constraints were fulfilled generally by ~95% of the atoms.

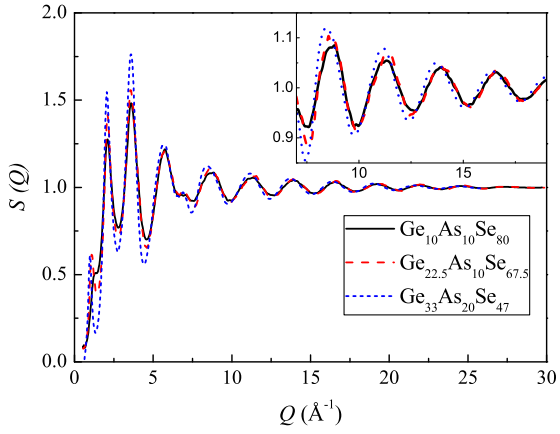

Fig. 1. X-ray diffraction structure factors of $Ge_{10}As_{10}Se_{80}$, $Ge_{22.5}As_{10}Se_{67.5}$ and $Ge_{33}As_{20}Se_{47}$.

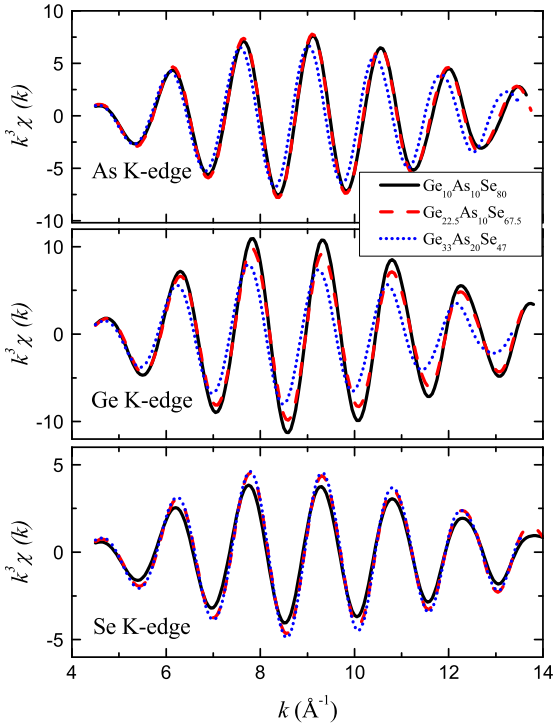

Fig. 2. Ge, As and Se K-edge $k^3\chi$ curves of $Ge_{10}As_{10}Se_{80}$, $Ge_{22.5}As_{10}Se_{67.5}$ and $Ge_{33}As_{20}Se_{47}$.

As only the 3 total coordination numbers (N_i) were fixed, the type of neighbors (N_{ij}) could vary within the limits allowed by the constraints. In a three-component system there are 6 independent N_{ij} values. Therefore the system has considerable freedom and N_{ij} values are fixed by the information content of the experimental data. Configurations obtained by using the 3 total coordination number constraints were used as references for assessing the validity of models applying various additional constraints.

The uncertainty of N_{ij} coordination numbers is around 0.3–0.4. This value was obtained by dedicated simulation runs, in which test coordination constraints were used to change systematically the given N_{ij}, starting from the values of the reference configurations. The cumulative relative R-factors (R_c) were used to quantify the overall quality of the fits. The R-factor of a given dataset (either EXAFS or X-ray diffraction) is defined by the following equation:

$$R = \frac{\sqrt{\sum_i (S_{\mathrm{mod}}(k_i) - S_{\mathrm{exp}}(k_i))^2}}{\sqrt{\sum_i S^2_{\mathrm{exp}}(k_i)}} \quad (1)$$

where S_{mod} and S_{exp} are the model and experimental structure factors (or EXAFS curves), k_i denotes the experimental points. Relative R-factors are obtained by dividing the given R-factor with that of

the R-factor of the same dataset in the reference model. We have selected the 'all bonds allowed' model as a reference for all compositions. Finally, R_c is given as the sum of the relative R-factors of the X-ray diffraction and EXAFS experiments divided by 4, the number of datasets fitted. Thus, R_c of the reference models is 1 by definition.

The uncertainty of bond lengths is about ±0.02 Å in case of mixed indices (Ge–As, Ge–Se, As–Se). These pairs directly contribute to two EXAFS spectra that keep their error at a relatively low level. The uncertainty of the distances of like atoms (Ge–Ge, As–As, Se–Se) is usually somewhat higher and depends strongly on the concentration of the given atom.

The quality of the fits is exemplified by Figs. 3 and 4 where the experimental and model XRD and EXAFS curves of $Ge_{27.5}As_{10}Se_{62.5}$ are compared. Partial pair correlation functions of the same composition are shown in Fig. 5. First peaks are well defined and very close to each other. (Nearest neighbor distances are within 0.10–0.13 Å for all compositions (Table 1).) The separation of so strongly overlapping peaks is possible only by combining the information provided by multiple experimental datasets.

4. Discussion

Nearest neighbor distances and coordination numbers of the Ge–As–Se glasses investigated are given in Tables 1 and 2, respectively. It can be observed that Ge–Ge, Ge–As or As–As bonds can be found even in strongly Se-rich alloys while Se–Se bonds persist in Se-poor compositions. (A glass with composition $Ge_xAs_ySe_{1-x-y}$ is Se-rich if $2(1-x-y) > 4x + 3y$. In case of equality the composition is stoichiometric, while it is Se-poor if $2(1-x-y) < 4x + 3y$). We carried out dedicated simulation runs to check whether the existence of the homonuclear Ge–Ge, As–As and Se–Se and heteronuclear Ge–As bonds is a simulation artefact or necessary to fit the experimental datasets. To achieve this goal we have created models in which these bonds were forbidden in various combinations.

4.1. Bonds between Ge and As in Se-rich glasses

The existence of Ge–Ge, Ge–As and As–As bonds was investigated in $Ge_{10}As_{10}Se_{80}$, the highest Se-content glass. R_c values of various models are given in Table 3. It was found that As–As bonding has a negligible effect on the quality of fits. The simultaneous elimination of As–As and Ge–Ge bonds results in a 5.7% increase of R_c. If all of Ge–Ge, Ge–As and As–As bonds were eliminated, R_c became as high as 1.29.

It can thus be concluded that in case of $Ge_{10}As_{10}Se_{80}$ As–As bonds are not needed to reproduce experimental data but fit quality drastically deteriorates if Ge–As bonds are eliminated. The reliability of this finding is also supported by the stability of Ge–As distance, which is 2.45–2.46 Å over the whole – very broad – composition range investigated (Table 1). This is the longest bond length, therefore the lack of Ge–As bonds cannot be compensated (without worsening fit quality) by an increase of other coordination numbers. On the other hand, As–As and Ge–Ge distances are somewhat more scattered suggesting that their fluctuations may be set off by changes in other distances.

We also note that $Ge_{10}As_{10}Se_{80}$ is strongly Se-rich, therefore elimination of bonds between minor components alone should not bring about drastic changes fit quality. The increase of R_c in the corresponding model clearly shows that Ge–As pairs are present in the glass.

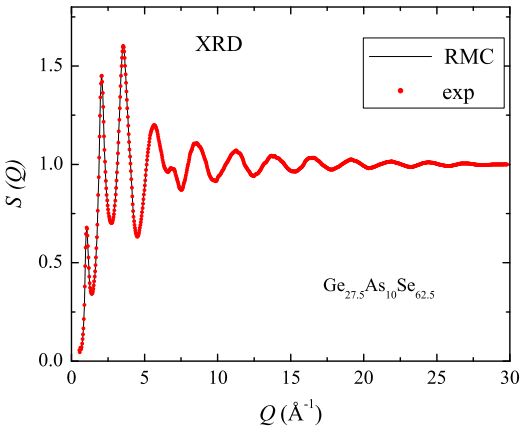

Fig. 3. X-ray diffraction fit of $Ge_{27.5}As_{10}Se_{62.5}$.

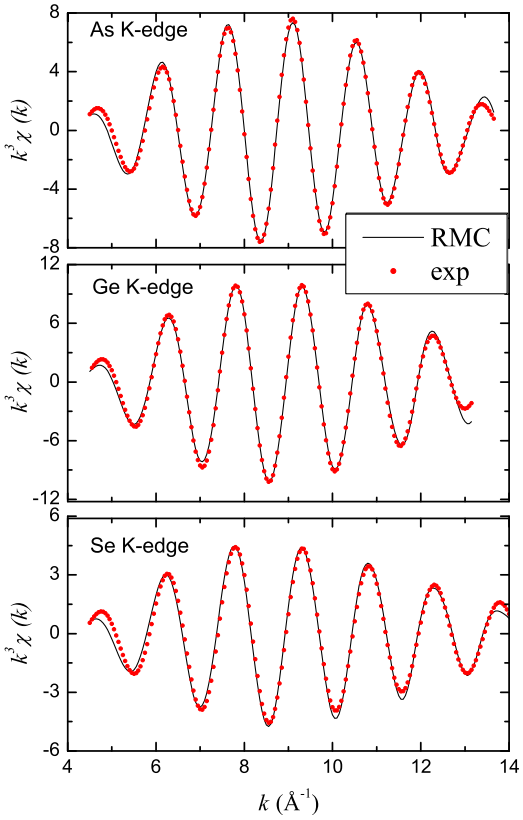

Fig. 4. Ge, As and Se K-edge EXAFS fits of $Ge_{27.5}As_{10}Se_{62.5}$.

4.2. Se–Se bonds in the strongly Se-deficient region

Models with and without Se–Se bonds were investigated to test whether Se–Se bonding is necessary to get a reasonable fit of experimental data of $Ge_{33}As_{20}Se_{47}$, the most Se-deficient glass. Se–Se bonding was eliminated by setting the corresponding minimum interatomic distance to 2.9 Å. It has been found that Se–Se bonds do improve the quality of the fit of Se K-edge EXAFS data even in this composition. The cumulative relative R-factor of the Se–Se bonding-free model was as high as 1.299. Fits of Se K-edge EXAFS data with and without Se–Se bonds are compared in Fig. 6.

4.3. Comparison with other IV–V–VI glasses

Detailed structural investigations of Ge–Sb–Te [35,36] and Ge–Sb–Se glasses [39] have shown that chalcogen-metal bonds have the highest priority and Ge/Sb–Ge/Sb bonds are formed only if there are no more available chalcogen atoms. The coordination numbers of $Ge_{22}As_{20}Se_{58}$ (also known as GASIR®) and $Ge_2Sb_2Te_5$

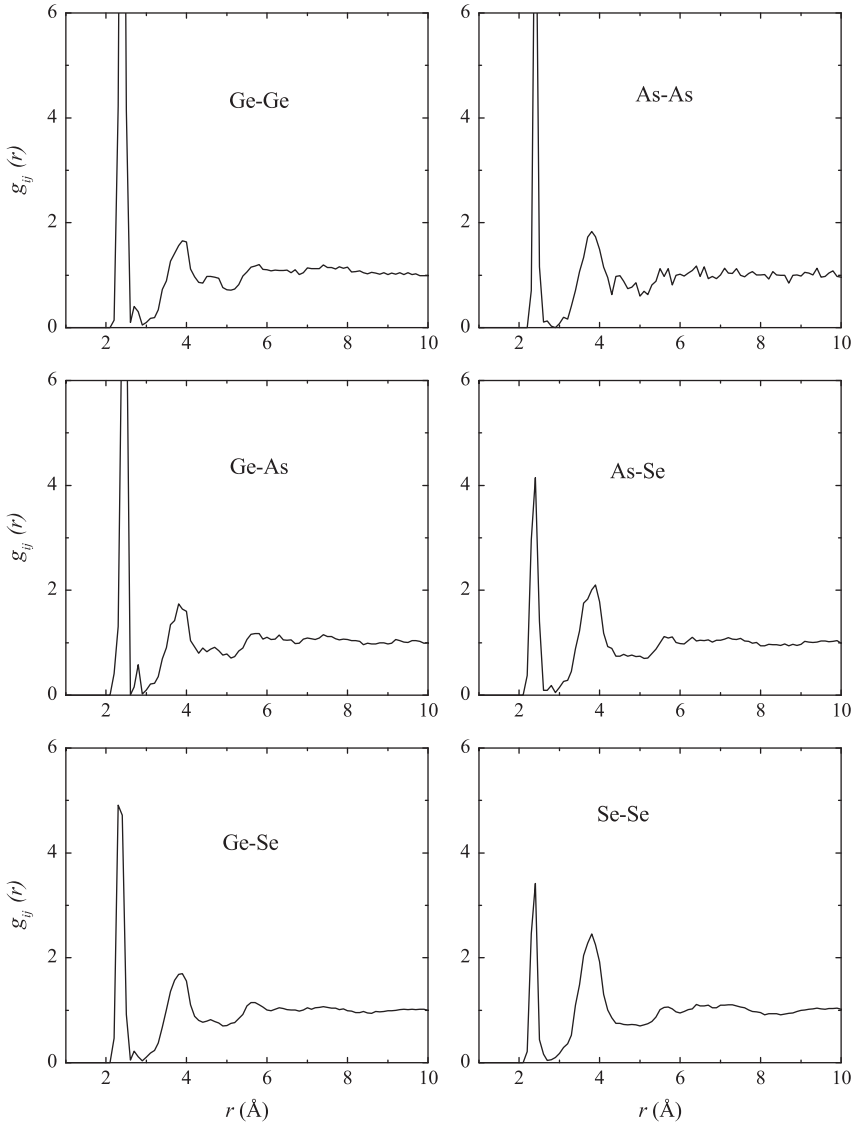

Fig. 5. Partial pair distribution functions of $Ge_{27.5}As_{10}Se_{62.5}$.

Table 1
Nearest neighbor distances in the Ge–As–Se glasses investigated.

Pair *i*–*j*	Alloy composition (concentration of Ge, As and Se in at.%)								
	10–10–80	17.5–10–72.5	22.5–10–67.5	22–20–58	27.5–10–62.5	30–10–60	33–12–55	35–10–55	33–20–47
Ge–Ge	2.39	2.42	2.36	2.38	2.40	2.37	2.39	2.42	2.41
Ge–As	2.45	2.46	2.45	2.45	2.45	2.46	2.46	2.46	2.46
Ge–Se	2.35	2.34	2.37	2.36	2.35	2.36	2.36	2.35	2.35
As–As	2.39	2.42	2.35	2.40	2.41	2.37	2.44	2.43	2.42
As–Se	2.39	2.36	2.39	2.39	2.37	2.37	2.38	2.38	2.37
Se–Se	2.35	2.37	2.33	2.35	2.36	2.33	2.33	2.37	2.37

are compared in Table 4, where the coordination numbers of the respective IV–V–VI random covalent networks are also given. In such a network N_{ij} coordination numbers are determined solely by the N_i total coordination numbers and the c_i atomic fractions of the constituents:

$$N_{ij} = \frac{c_j N_i N_j}{\sum c_k N_k} \tag{2}$$

It can be observed that $Ge_2Sb_2Te_5$ is characterized by pronounced chemical short range order: Te–Te bonds are absent and Ge/Sb–Ge/Sb bonds are formed only in the absence of free Te atoms. On the other hand, coordination numbers of $Ge_{22}As_{20}Se_{58}$ do not deviate significantly from the corresponding values of the random covalent network. In Table 2 the random values are given for all compositions (values in parentheses). In most cases they agree with the experiment-based values within their uncertainty, showing the lack of strong chemical ordering in Ge–As–Se glasses.

This observation is in contrast with the behavior of other IV–V–VI glasses. Various experimental studies revealed that chemical ordering is very pronounced in the Ge–As–S system as well. Sen et al. investigated the structure of $Ge_xAs_yS_{1-x-y}$ glasses with x:y = 1:2, 1:1, and 2.5:1 over a wide-ranging S content [40]. It

Table 2
Coordination numbers of the Ge–As–Se glasses investigated. The values of the corresponding random covalent networks are given in parentheses (see Section 4.3).

Pair *i*–*j*	Alloy composition (concentration of Ge, As and Se in at.%)								
	10–10–80	17.5–10–72.5	22.5–10–67.5	22–20–58	27.5–10–62.5	30–10–60	33–12–55	35–10–55	33–20–47
Ge–Ge	1.07(0.70)	1.34(1.14)	1.68(1.41)	1.46(1.33)	1.84(1.66)	2.04(1.78)	1.96(1.90)	2.18(2.00)	1.93(1.85)
Ge–As	0.62(0.52)	0.59(0.49)	0.52(0.47)	0.88(0.91)	0.47(0.45)	0.45(0.44)	0.52(0.52)	0.43(0.43)	0.86(0.84)
Ge–Se	2.35(2.78)	2.11(2.37)	1.82(2.12)	1.69(1.76)	1.72(1.89)	1.53(1.78)	1.55(1.58)	1.41(1.57)	1.24(1.31)
As–Ge	0.62(0.52)	1.03(0.86)	1.18(1.06)	0.96(1.00)	1.30(1.25)	1.35(1.33)	1.43(1.42)	1.51(1.50)	1.42(1.38)
As–As	0.32(0.39)	0.41(0.37)	0.36(0.35)	0.66(0.68)	0.30(0.34)	0.39(0.33)	0.36(0.39)	0.28(0.32)	0.57(0.63)
As–Se	2.16(2.09)	1.65(1.76)	1.49(1.59)	1.41(1.32)	1.42(1.42)	1.25(1.33)	1.23(1.19)	1.23(1.18)	0.99(0.99)
Se–Ge	0.29(0.35)	0.51(0.57)	0.61(0.71)	0.64(0.67)	0.76(0.83)	0.77(0.89)	0.93(0.95)	0.90(1.00)	0.87(0.92)
Se–As	0.27(0.26)	0.23(0.24)	0.22(0.24)	0.48(0.45)	0.23(0.23)	0.21(0.22)	0.27(0.26)	0.22(0.21)	0.42(0.42)
Se–Se	1.49(1.39)	1.34(1.18)	1.16(1.06)	0.93(0.88)	1.02(0.94)	1.00(0.89)	0.83(0.79)	0.86(0.79)	0.66(0.66)
MCN	2.30	2.45	2.55	2.64	2.65	2.70	2.78	2.80	2.86
Se-rich/poor	+0.45	+0.225	+0.075	−0.16	−0.075	−0.15	−0.29	−0.3	−0.49

Table 3
Cumulative relative *R*-factors (see the text for definition) of various models of $Ge_{10}As_{10}Se_{80}$.

Model	Reference model	As–As forbidden	As–As and Ge–Ge forbidden	As–As, Ge–Ge, Se–Se and Ge–As forbidden
R_c	1.000	1.005	1.057	1.292

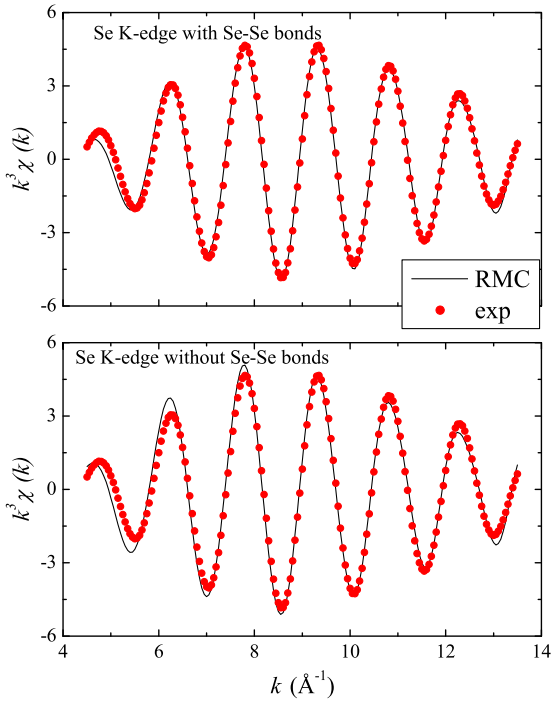

Fig. 6. Se K-edge EXAFS fits of $Ge_{33}As_{20}Se_{47}$ glass with and without Se–Se bonds.

was found that upon decreasing the S content first As–As bonds appear, while Ge takes part in metal–metal bonds only in strongly S-poor compositions. A combined neutron and X-ray diffraction study of $Ge_xAs_xS_{100-2x}$ glasses [41] gave similar conclusions.

The structure of Ge–As–Te glasses has also been investigated by the combination of diffraction techniques, EXAFS and reverse Monte Carlo simulation [42]. It has been reported that Te–Te bonds can be found in strongly Te-deficient compositions while As–As bonds exist in Te-rich glasses. On the other hand, Ge–Ge bonding seems to be avoided even in Te-poor compositions which is a clear sign of chemical ordering around Ge. In view of these findings the complete lack of chemical short range order in Ge–As–Se glasses should be regarded as an anomaly.

4.4. Chemical short-range order and optical nonlinearity

The physical properties of Ge–As–Se glasses have been shown to vary remarkably with either the Ge-concentration or the theoretical mean coordination number [43,44]. For example, the nonlinear refractive index n_2 of the Ge–As–Se glasses plotted as a function of the mean coordination number exhibits a minimum at the MCN values of about 2.7–2.8 [44] (Fig. 7a). It has been shown in [24] that there is a correlation between the behavior of the nonlinear refractive index and the total number of Ge–Ge, As–As, Se–Se and Ge–As bonds in $Ge_5As_xSe_{95-x}$ and $Ge_{15}As_xSe_{85-x}$ glasses. In the present study we have calculated the fractions of the above bonds (denoted with φ_{ij}) in the $Ge_xAs_{10}Se_{90-x}$ series and plotted $\varphi_{GeGe} + \varphi_{GeAs}$ and φ_{SeSe} as a function of the mean coordination number in Fig. 7b. For each constituent, φ_{ij} has been determined as a ratio of the respective bonds ($c_i N_{ij}$) to N_i, the total number of bonds in the simulation box:

$$\varphi_{ij} = \frac{c_i N_{ij}}{N_i} \tag{3}$$

There is a good agreement in the dependences of the nonlinear refractive index n_2 and the total fraction of Ge–Ge, As–As, Se–Se and Ge–As bonds φ_{tot} (compare Fig. 7a and b). This supports the suggestion of Harbold et al. [45] that the nonlinearity is influenced by both the presence of unpaired electrons and defect states in glasses. Indeed, the lone electron pairs may play a dominant role for achieving large nonlinearities in the Se-rich glasses where the

Table 4
Comparison of the coordination numbers of $Ge_{22}As_{20}Se_{58}$ and $Ge_2Sb_2Te_5$ [36] with those of the respective IV–V–VI random covalent networks (in parentheses).

	Ge–Ge	Ge–As/Ge–Sb	Ge–Se/Ge–Te	As–As/Sb–Sb	As–Se/Sb–Te	Se–Se/Te–Te
$Ge_{22}As_{20}Se_{58}$	1.46 (1.33)	0.88 (0.89)	1.69 (1.78)	0.66 (0.68)	1.41 (1.32)	0.93 (0.88)
$Ge_2Sb_2Te_5$	0.79 (1.33)	0.60 (1.0)	2.45 (1.67)	0 (0.75)	2.53 (1.25)	0 (0.83)

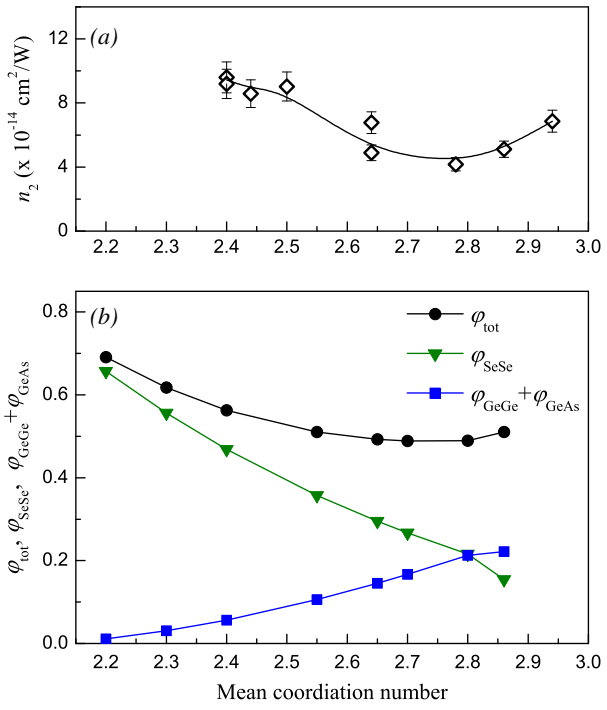

Fig. 7. (a) Nonlinear refractive index n_2 of the Ge–As–Se glasses measured at 1500 nm [44]; (b) fraction of different bonds in the $Ge_xAs_{10}Se_{90-x}$ glasses. To extend the mean coordination number region values of $Ge_{33}As_{20}Se_{47}$ are also shown (highest MCN); φ_{SeSe} – Se–Se bonds, φ_{GeGe} + φ_{GeAs} – Ge–Ge and Ge–As bonds, φ_{tot} – total fraction of Ge–Ge, As–As, Se–Se and Ge–As bonds. The lines are guides for the eye.

fraction of Se–Se bonds is large (triangles in Fig. 7b), whereas Ge–Ge and Ge–As bonds (squares in Fig. 7b) may contribute to the increasing nonlinearity in Se-poor glasses.

5. Summary

The structure of several Ge–As–Se glasses with mean coordination numbers between 2.20 and 2.86 has been investigated by X-ray diffraction and EXAFS at the Ge, As and Se K-edges. Structural models have been obtained by fitting the experimental datasets by the reverse Monte Carlo simulation technique. It has been found that various bonds between Ge and As (Ge–Ge, As–As, As–Ge) exist in Se-rich compositions while Se–Se bonds persist in strongly Se-deficient alloys. Unlike other IV–V–VI glass systems (e.g. Ge–As–S, Ge–As–Te, Ge–Sb–Te, Ge–Sb–Se) there is no significant chemical short range order in Ge–As–Se glasses.

Acknowledgments

This research was partly supported by the Australian Research Council through its Centres of Excellence and Discovery (DP110102753) programs. P. Jóvári is indebted to the Hungarian Basic Research Fund (OTKA) for financial support (Grant No. 083529).

References

[1] A.R. Hilton, Chalcogenide Glasses for Infrared Optics, McGraw-Hill, New York, 2010.
[2] J.S. Sanghera, I.D. Aggarwal, J. Non-Cryst. Solids 256 (1999) 6.
[3] M. Asobe, Opt. Fiber Technol. 3 (1997) 142.
[4] V.S. Shiryaev, M.F. Churbanov, J. Non-Cryst. Solids 377 (2013) 225.
[5] G. Snopatin, V.S. Shiryaev, V.G. Plotnichenko, E.M. Dianov, M.F. Churbanov, Inorg. Mater. 45 (2009) 1439.
[6] C. Vigreux, M. Vu Thi, R. Escalier, G. Maulion, R. Kribich, A. Pradel, J. Non-Cryst. Solids 377 (2013) 205.
[7] S.D. Jackson, G. Anzueto-Sanchez, Appl. Phys. Lett. 88 (2006) 221106.
[8] T. Kohoutek, X. Yan, T.W. Shiosaka, S.N. Yannopoulos, A. Chrissanthopoulos, T. Suzuki, Y. Ohishi, J. Opt. Soc. Am. B 28 (2011) 2284.
[9] M.L. Anne et al., Sensors 9 (2009) 7398.
[10] B. Bureau et al., J. Non-Cryst. Solids 345 (2004) 276.
[11] A. Ganjoo, H. Jain, C. Yu, R. Song, J.V. Ryan, J. Irudayaraj, Y.J. Ding, C.G. Pantano, J. Non-Cryst. Solids 352 (2006) 584.
[12] J. Keirsse, C. Boussard-Pledel, O. Loreal, O. Sire, B. Bureau, B. Turlin, P. Leroyer, J. Lucas, J. Non-Cryst. Solids 326 (2003) 430.
[13] A. Seddon, Int. J. Appl. Glass Sci. 2 (2011) 177.
[14] F. Charpentier, B. Bureau, J. Troles, C. Boussard-Pledel, K. Michel-Le Pierres, F. Smektala, J.L. Adam, Opt. Mater. 31 (2009) 496.
[15] S. Maurugeon, B. Bureau, C. Boussard-Pledel, A.J. Faber, X.H. Zhang, W. Geliesen, J. Lucas, J. Non-Cryst. Solids 355 (2009) 2074.
[16] J. Phillips, J. Non-Cryst. Solids 34 (1979) 153.
[17] M. Thorpe, J. Non-Cryst. Solids 57 (1983) 355.
[18] K. Tanaka, Phys. Rev. B 39 (1989) 1270.
[19] R.P. Wang, A. Smith, B. Luther-Davies, H. Kokkonen, I. Jackson, J. Appl. Phys. 105 (2009) 056109.
[20] R.P. Wang, A. Smith, A. Prasad, D.Y. Choi, B. Luther-Davies, J. Appl. Phys. 106 (2009) 043520.
[21] M.F. Thorpe, D.J. Jacobs, M.V. Chubynsky, J.C. Phillips, J. Non-Cryst. Solids 266 (2000) 859.
[22] P. Boolchand, G. Lucovsky, J. Phillips, M. Thorpe, Philos. Magn. 85 (2005) 3823.
[23] Y. Wang, P. Boolchand, M. Micoulaut, Euro Phys. Lett. 52 (2000) 633.
[24] I. Kaban, P. Jóvári, R.P. Wang, B. Luther-Davies, N. Mattern, J. Eckert, J. Phys.: Condens. Matter 24 (2012) 385802.
[25] R.L. McGreevy, L. Pusztai, Mol. Simulat. 1 (1988) 359.
[26] R.L. McGreevy, J. Phys.: Condens. Matter 13 (2001) R877.
[27] O. Gereben, P. Jóvári, L. Temleitner, L. Pusztai, J. Optoelectron. Adv. Mater. 9 (2007) 3021.
[28] T. Wang, W.H. Wei, X. Shen, R.P. Wang, B. Luther-Davies, I. Jackson, J. Phys. D: Appl. Phys. 46 (2013) 165302.
[29] N. Schell, A. King, F. Beckmann, T. Fischer, M. Müller, A. Schreyer, Mater. Sci. Forum 772 (2014) 57.
[30] A.P. Hammersley, S.O. Svensson, M. Hanfland, A.N. Fitch, D. Häusermann, High Press. Res. 14 (1996) 235.
[31] Y. Waseda, The Structure of Non-Crystalline Materials, McGraw-Hill, New York, 1980.
[32] S.J. Gurman, R.L. McGreevy, J. Phys.: Condens. Matter 2 (1990) 9463.
[33] M. Winterer, J. Appl. Phys. 88 (2000) 5635.
[34] N. Mott, Adv. Phys. 16 (1967) 49.
[35] P. Jóvári, I. Kaban, J. Steiner, B. Beuneu, A. Schöps, M.A. Webb, Phys. Rev. B 77 (2008) 035202.
[36] P. Jóvári, I. Kaban, J. Steiner, B. Beuneu, A. Schöps, A. Webb, J. Phys.: Condens. Matter 19 (2007) 335212.
[37] S. Sen, B.G. Aitken, Phys. Rev. B 66 (2002) 134204.
[38] I. Petri, P.S. Salmon, H.E. Fischer, Phys. Rev. Lett. 84 (2000) 2413.
[39] W.-H. Wei, R.-P. Wang, X. Shen, L. Fang, B. Luther-Davies, J. Phys. Chem. C 117 (2013) 16571.
[40] S. Sen, C.W. Ponader, B.G. Aitken, Phys. Rev. B 64 (2001) 104202.
[41] S. Uzun, S. Sen, C.J. Benmore, B.G. Aitken, J. Phys.: Condens. Matter 20 (2008) 335105.
[42] P. Jóvári, P. Lucas, Z. Yang, B. Bureau, I. Kaban, B. Beuneu, J. Bednarcik, J. Am. Ceram. Soc. 97 (2014) 1625.
[43] B. Luther-Davies, Z. Congji, A. Prasad, A. Smith, Conference on Lasers and Electro-Optics/Quantum Electronics and Laser Science Conference and Photonic Applications Systems Technologies, OSA Technical Digest Series (CD), Optical Society of America, paper CMGG7, 2007. doi:10.1109/CLEO.2007.4452537.
[44] A. Prasad, C.-J. Zha, R.-P. Wang, A. Smith, S. Madden, B. Luther-Davies, Opt. Express 16 (2008) 2804.
[45] J.M. Harbold, F.Ö. Ilday, F.W. Wise, J.S. Sanghera, V.O. Nguyen, L.B. Shaw, I.D. Aggarwal, Opt. Lett. 27 (2002) 119.